Solid State Communications, Vol.61,No.3, pp.187-192, 1987.
Printed in Great Britain.

0038-1098/87 $3.00 + .00
Pergamon Journals Ltd.

SPIN-RESOLVED PHOTOEMISSION FROM Ir(111): TRANSITIONS INTO A SECONDARY BAND AND ENERGETIC POSITION OF THE FINAL STATE BANDS

N. Müller, B. Kessler, B. Schmiedeskamp, G. Schönhense and U. Heinzmann

Universität Bielefeld, Fakultät für Physik, D-4800 Bielefeld
and
Fritz-Haber-Institut der MPG, D-1000 Berlin 33

(Received October 1st, 1986 by P. Wachter)

Spin resolved photoelectron spectroscopy with Ir(111) was performed in normal incidence of circularly polarized VUV radiation and normal electron emission. Using the spin information the spectra were separated with regard to the symmetry of the initial states. Besides the dominant transitions into the free electron like parts of the unoccupied bands, transitions into a secondary unoccupied band were unambiguously identified. Transitions into this secondary band cannot be evidenced without spin analysis. The data are in excellent agreement with a fully relativistic first-principles band structure calculation of Noffke and Fritsche, except for an overall shift of $\Delta\varepsilon$ = 0.8 eV ±0.3 eV for the energy of the unoccupied final bands.

1. Introduction

In electronic transitions caused by circularly polarized photons the electron spins are commonly aligned. This is also true for unpolarized targets (1-7). This alignment arises from the spin-orbit interaction. For direct transitions the resulting electron spin polarization (ESP) is determined by the symmetry of the states involved, and is described by the corresponding (relativistic) selection rules for optical dipole transitions.

The detectability of the spin effects depends on the magnitude of the resulting spin-orbit energy splitting in comparison to both the lifetime broadening of the excited electronic states and the experimental resolution. For medium- and high-Z materials the spin-orbit coupling is strong, and compared to the detectability limits the electronic states are split and/or modified considerably. Correspondingly, the nonrelativistic selection rules, which only account for the spatial symmetry, break down while the relativistic ones (which include spin) persist (8). With solids, a spin resolved photoemission experiment thus yields information not obtainable without accounting for spin effects, namely about the symmetry and the hybridization of the states involved (5,6,9-12).

In photoemission from solids via non hybridized final states with normally incident circularly polarized light and normal emission along a high symmetry line (i.e. in cubic crystals along Λ or Δ), electrons arising from one distinct direct transition are totally polarized parallel or antiparallel to the photon polarization. The sign of the spin polarization (13) depends only on the symmetry of the initial state involved and the helicity of the incident light (9,10), as the final states must be totally symmetric for the case of normal emission (14).

The resulting photoelectron intensity spectra should thus consist of two partial spectra correlated to transitions characterized by P = +1 or P = -1. These partial spectra I_+ and I_- are related to the measured total intensity I and the measured spin polarization P by

$$I_+ = \frac{1}{2}I(1+P) \text{ and } I_- = \frac{1}{2}I(1-P) \qquad (1).$$

Structures which are superimposed in the total intensity I may then be separated in the partial intensities I_+ and I_- thus giving an improved identification and localization of peaks. This procedure separates the spin-orbit split initial states. The separation is not attainable by using linearly polarized light, since the spin dependent effects occur only due to the definite phase relations in the coupling of the x- and y-component of circularly polarized light (9,10). Using linearly polarized light it is only possible to separate initial states of different spatial symmetry as long as they are not mixed by spin-orbit coupling (14,8). The intensity separation given in eq. (1) has been successfully applied before in photoemission from magnetized materials to distinguish transitions originating from majority and minority spin bands (15,16), and in a previous spin resolved photoemission study of Pt(111) (11) as well as in spin polarized LEED (17).

In this paper we use partial intensities obtained in a spin-resolved photoemission experiment to investigate details of the Ir band structure along $\Gamma\Lambda L$, and to perform a cross comparison with the relativistic band structure calculation of Ir given by Noffke and Fritsche (18) (NF, see Fig. 1).

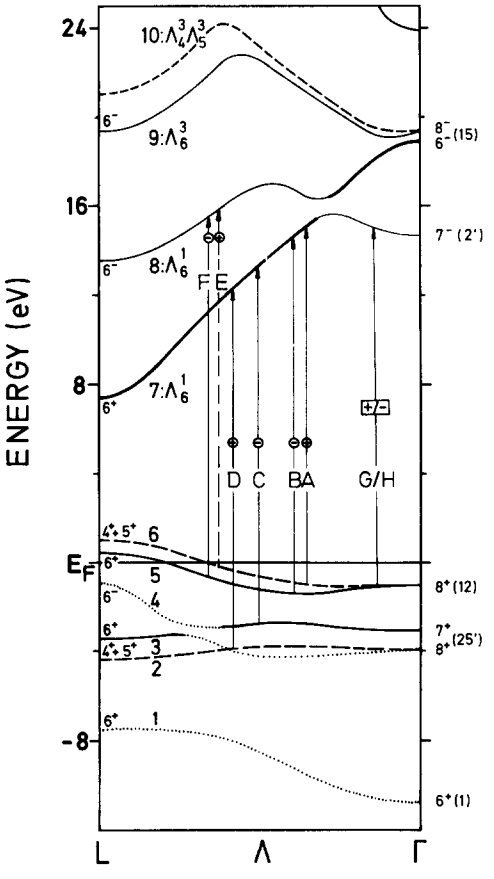

Fig. 1. Bandstructure of Ir along ΓL caiculated by Noffke and Fritsche (NF) [18]. In the occupied bands the line types characterize the symmetry of the states: Λ_6^1 ··· , Λ_6^3 ——, $\Lambda_4^3 + \Lambda_5^3$---. The solid arrows are transitions assigned by NF (A,B,C,D,F,G,H); transition E is drawn for completion. The signs inserted into the arrows indicate the sign of the spin polarization of electrons excited by σ^+ lignt. They follow from the relativistic dipole selection rules given by Wöhlecke and Borstel [9]. The parts of bands 7 and 8 marked by heavy lines are "free electron like".

To interpret the structures apparent in photoemission spectra measured by van der Veen et al. [19] (VHE) NF have considered not only the transitions into the free electron like segments of the unoccupied bands 7 and 8 between L_{6+} and Γ_{6-} (see Fig. 1, transitions A, B, C, and D) but also transitions to the remaining parts of the bands 7 and 8 (Fig. 1, transitions (E), F and G/H). These transitions to secondary bands (secondary cones [20]) should be negligible due to the finite lifetime of the excited electronic states [21]. Furthermore, the corresponding structure measured by VHE is only a shoulder between E and the peak arising from transition A. As VHE have used partly p-polarized light this shoulder could also be explained by surface state emission.

One purpose of this paper is to identify the transitions E, F and G/H by means of spin-dependent partial intensities. A second is to prove the energetic position of the unoccupied bands 7 and 8. While the calculation of NF reproduced most values for the positions of critical points measured by VHE within the experimental uncertainties, the L_{6-} point of band 8 was calculated to be 0.5 eV lower in energy. Further discrepancies in critical point energies were observed by Mack et al. [22]. They have found secondary electron emission structures correlated with L_{6-} and a resonant photoemission peak related to the flat band region near Γ_{6-} lying about 0.7 eV higher in energy than calculated by NF.

2. Experimental

The measurements were performed at the electron storage ring BESSY using the circularly polarized off-plane radiation monochromatized by a 6.5 m normal incidence monochromator [23].

The bandwidth of the light was 0.5 nm, the degree of circular polarization (88 ±3)% [24]. The direction of light incidence coincided with the Ir(111) surface normal within 0.3°. Photoelectrons emitted in an acceptance half angle of 3° around the surface normal were collected by a simulated hemispherical energy analyzer [25] followed by an UHV Mott-detector for ESP analysis. The energy analyzer was operated with constant pass energy resulting in an energy resolution < 150 meV independent of the initial energy. Apparatus asymmetries of the Mott-detector are eliminated by changing the helicity of the light.

The Ir(111) crystal surface was aligned within 0.1° using an x-ray diffractometer, ground on SiC (mesh 600 - 800) and polished with diamond paste in successive steps from 50 μ to 0.25 μ. The crystal was held by Ir wires lying in spark-cut grooves and was mounted on top of a liquid He cooled target manipulator. Heating was performed by electron bombardment using an Ir/ThO low temperature filament. The heating temperature was controlled by a W/Ir thermocouple [26].

Characterization of the Ir(111) surface was done in situ by Auger spectroscopy and LEED. The clean surface was prepared by Ne^+ bombardment and by repeated cycles of heating in oxygen at about 1100 K and by flashing to about 1400 K. The oxygen was admitted using a doser giving a partial pressure of about 10^{-6} mbar in front of the crystal. To minimize phonon effects [27] during the measurements the crystal temperature was held at about 60 K which is about 14% of the Ir Debye-temperature Θ_D = 420 K [28].

3. Results and Discussion

A typical set of data obtained by spin resolved photoemission is presented in Fig. 2. From the total intensity I (upper panel) and the corresponding polarization P (middle panel) measured for an excitation energy hν = 16 eV the partial intensities I_+ and I_- were obtained using equation (1) (lower panel). I_+ and I_- illustrate the improved distinction of the

peaks in the spin-resolved photoemission spectra compared to the total intensity I.

Four dominant peaks labelled A, B, C, and D are resolved in the total intensity I as well as in the partial intensities I_+ and I_-. I_+ and I_- demonstrate that as in the case of Pt(111) A, B, C, and D are correlated to transitions yielding totally polarized electrons; the sign of P serves to assign these transitions doubtlessly to the occupied bands 6, 5, 4, and 2 (see Fig. 1). It is worth noting that the degree of polarization $|P|$ of up to 80% (as shown in the middle panel of Fig. 2) exceeds all data previously measured for nonmagnetic 3D crystals.

Besides the peaks A, B, C, and D in the total intensity a weak shoulder exists near E_F. This shoulder is correlated with a pronounced structure in the spin polarization and appears as a clearly resolved peak in the I_--spectrum. This peak (shoulder) originates from a transition F between bands 5 and 8, as postulated by NF. To verify the assignment of transition F more extensively, and to look for a transition E from band 6 to band 8 as well as for the transitions G/H from 5/6 to 7 near Γ, we have taken spectra at several photon energies $h\nu$ between 14.8 eV and 17.8 eV and obtained the spin-resolved results presented in Fig. 3.

While the total intensities, which are again dominated by the peaks A, B, C, and D, do not reveal well defined transitions E, F and their expected dispersion, the partial intensities I_+ and I_- do so. Thus the existence of the transitions E and F going from band 6 and 5 (symmetry $\Lambda_4^3 + \Lambda_5^3$ and symmetry Λ_6^3) to band 8 (symmetry Λ_6^1) is demonstrated by identifying the corresponding peaks in the partial intensities I_+ and I_-, respectively. The thresholds for the appearance of the peaks E and F are $h\nu$ = 16.4 eV ±0.1 eV and $h\nu$ = 15.1 eV ±0.1 eV, respectively. They are deduced from the data using the constant initial state method given by Knapp et al. (29). With these thresholds found for E and F two points of the final state band 8 can be fixed in the band structure $\varepsilon(k)$ using the fermi level crossing method (29). As there are no de Haas - van Alphen data for the fermi level crossing points of bands 5, 6 along $\Gamma\Lambda L$ in Ir, we use the level crossings given by NF and perform thus a check of the calculated band structure. The result is presented in Fig. 4: band 8 has to be shifted by 0.8 eV ±0.3 eV towards higher energies. The uncertainty of ±0.3 eV is estimated taking into account the uncertainty of the monochromator calibration (~0.15 eV) and the error of the threshold determination. This energy shift may be due to an essential difference between measurement and calculation: The measured energies are excitation energies $\tilde{\varepsilon}$ (real parts of the quasi-particle energies), the calculated energies are ground-state one particle energies ε (30). The difference $\tilde{\varepsilon}-\varepsilon$ has to be zero at E_F (31). The value of +0.8 eV is reasonable for metals at $\tilde{\varepsilon}-E_F \approx 15$ eV (30,32).

The shift of band 8 to higher energies is supported by structure J (see Fig. 3): Starting at about $h\nu$ = 17 eV at the low energy side of peak C a shoulder J is growing. At $h\nu$ = 17.6 eV it forms a double peak together with peak C, the separation of C and J being about 0.5 eV. The peak J is present only in the partial intensity I_-, as for peak C. Thus both J and C are due to a direct transition $\Lambda_6^3 \rightarrow \Lambda_6^1$ with P = -1. Hence J must be assigned to be the onset of a transition from band 3 to band 8 near L (see Fig. 4). It cannot be assigned to a secondary electron structure

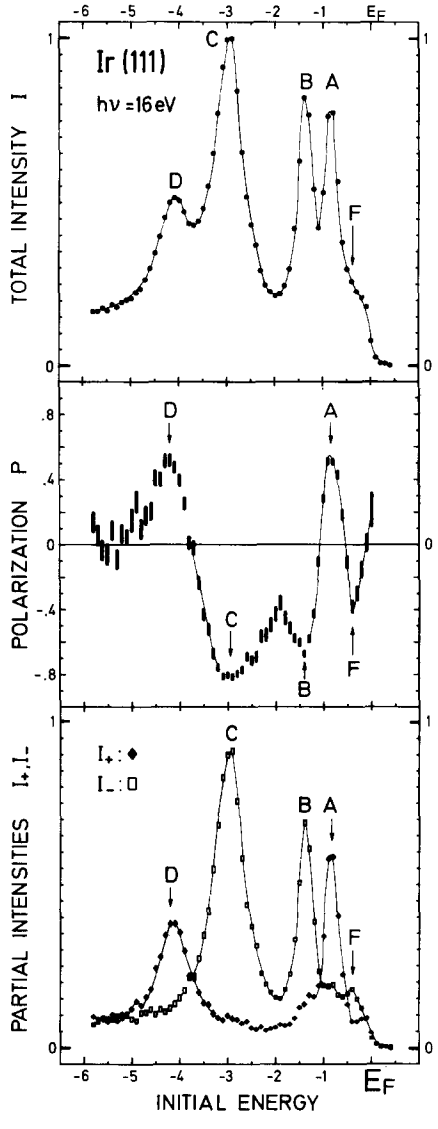

Fig. 2. Total intensity I (upper panel), electron spin polarization P (middle panel) and partial intensities I_+, I_- (lower panel) measured at a photon energy $h\nu$=(16.0 ±0.15) eV. For P, the error bars give the statistical uncertainty (1 x σ due to particle counting). There is an additional scaling error of ±10% due to calibration uncertainties of the light polarization and of the Mott-detector. For I_+, I_- the hight of the symbols gives the statistical error. The additional uncertainty due to the scaling of P is omitted, it has no effect on the results. The total intensity has been measured independently of the polarization.

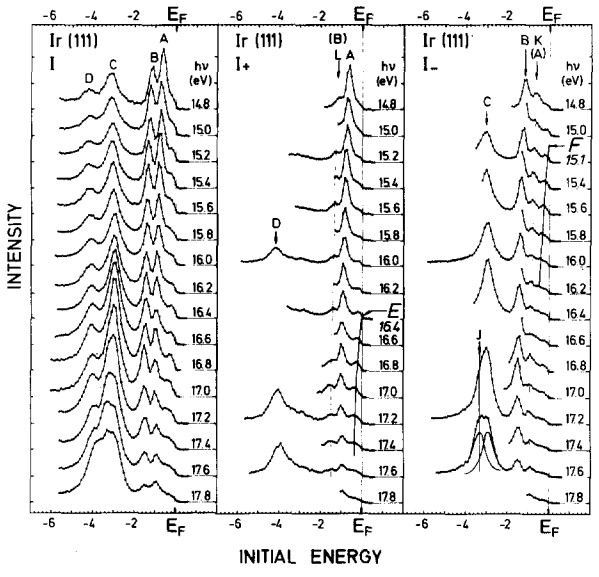

Fig. 3. Total intensity (first panel), partial intensity I_+ (second panel), and partial intensity I_- (third panel) measured at various photon energies from 14.8 eV to 17.8 eV. The given points are larger than the statistical errors (see. Fig. 2). The structures discussed in the text and the thresholds for transitions E and F are marked.

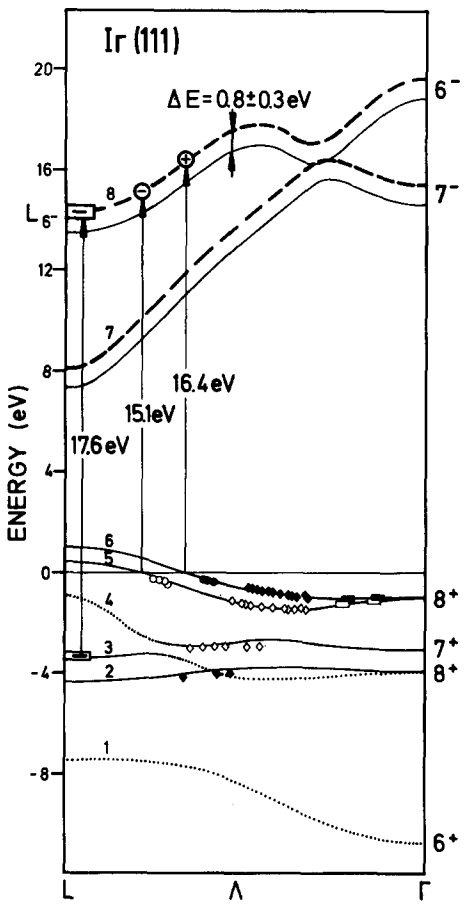

Fig. 4. Bandstructure of Ir along ΓL and results of our measurements. The solid and dotted lines represent the band structure calculated by Noffke and Fritsche (NF) (18). The broken lines give the unoccupied bands shifted to higher energies by ΔE = (0.8 ±0.3) eV. The mapping points marked by circles (●,○) correspond to transitions into band 8, the points marked by rhombs (◆,◇) to transitions into band 7. The mapping points near Γ marked by rectangles (▬,▭) are taken from measurements at hν=19 eV and hν=20 eV not presented in Fig. 3. Filled symbols represent P > 0, open symbols P < 0. Transitions starting at the dotted bands (symmetry Λ_6^1) are not allowed for the geometry used in this work.

correlated with the critical point L_{6^-} of band 8, as a secondary electron structure would show P ≃ 0. Transition J results in an energetic position of L_{6^-} at 14.2 eV ±0.3 eV, compared to the value of 13.54 eV calculated by NF. This difference is in accordance with the energetic shift of 0.8 eV ±0.3 eV given above. It is remarkable that the peaks J and C are of comparable intensity. On the basis of intensity calculations for normal photoemission from Ag(111) (33) and Au(111) (34), the transition J should not be measurable due to a vanishing surface transmission factor.

The transitions G and H from bands 5 and 6 to band 7 near Γ (see Fig. 1) cannot be identified in the total intensity spectra. The I_--spectrum shows up a structure K close to the expected position for G/H, but K also exists below the threshold for G/H (15.6 eV). The dispersion of K is equivalent to the dispersion of peak A which in addition is inconsistent with the existence of G/H. The I_+-spectrum also shows up a peak L, which disperses like peak B. Both peaks K and L are significant and cannot be removed by considering systematic uncertainties of the measurements. These peaks may be due to the weak hybridization resulting from a mixing of band 7 with bands of the same double group symmetry Λ_6 lying higher in energy, e.g. band 9 (see Fig. 1). Besides the spatial parts of the spinors transforming like Λ_1 the wavefunctions of band 7 (and 8) contain a few percent of spatial parts transforming like Λ_3 (35). Assuming appropriate matrix elements the structures K and L then must exist, and be strongly related to the structures A and B.

Our measurements given in Fig. 3 allow a further test of the band structure calculation by NF. As the calculation gives small energy differences between neighbouring bands much more accurately than large bandgaps (the quasi-particle correction varies slowly with energy), it is reasonable to shift band 7 also towards higher energies by 0.8 eV as experimentally found for band 8. Taking into account this shift the use of the final state band structure calculation in connection with the spin-resolved partial intensity spectra allows a symmetry resolved mapping of the occupied bands. The mapping points resulting from the transitions A, B, C, and D to band

7 are included in Fig. 4 together with those from the transitions E and F to band 8. They agree with the calculated bands within the experimental uncertainties. (The systematic calibration error of the photon energy is cancelled in this procedure). Some systematic shifts of 0.1 to 0.2 eV to lower energies are, however, found for bands 2 and 4. These shifts may also be due to quasi-particle corrections. But ground state one particle calculations are exact only within the limits given by the observed shift [30].

4. Conclusions

Transitions into a secondary unoccupied band have been identified and symmetry characterized by spin-polarization measurements. This is not easily possible by use of the photoelectron intensity alone [36]. The spin resolved band mapping procedure yields excellent agreement with the NF bandstructure calculation in the occupied d-bands as well as in the unoccupied final bands if the latter are shifted in energy by 0.8 eV compared with theory.

Several properties of Ir(111) have facilitated the derivation of the results presented. The high Debye temperature of 420 K [28] yields a small broadening of photoemission peaks due to thermal vibrations. Also, the (occupied) d-bands energetically lie close to E_F resulting in a weak hole lifetime broadening. This is especially true for the two upper d-bands (5 and 6), see Figs. 1,4) which cross the Fermi level. Compared to other crystals (e.g. Pt(111) [5,37]) it is a further advantage of Ir(111) that the emission of these bands cannot be superimposed by surface emission from other directions with high density of states (i.e. the Q- or Z-direction) because the corresponding flat bands lie above E_F [18]. It should also be noted that Ir(111) constitutes one of the rare examples of a non-reconstructed surface and that the preparation of the clean surface is possible without complications (partly a consequence of the high melting point T_M = 2410°C). Ir(111) can thus serve as a model target for photoemission from high-Z materials, especially under the aspect of spin resolved photoelectron spectroscopy.

Acknowledgements - The authors wish to thank Mrs. Eichele, G. Neff, E. Umbach (TU München) and Mrs. Tangermann (LMU München) for help in the preparation of the Ir(111) crystal. The crystal was kindly provided by T. Rhodin (Cornell University) and by B. Addiss (Materials Preparation Lab., Materials Sciences Center, Cornell University). We are grateful to F. Noffke and L. Fritsche (TU Clausthal) for providing details of the Ir band structure. We thank M. Wöhlecke, M. Neumann, G. Borstel, and K. Snowdown (Universität Osnabrück) for a critical reading of the manuscript and for helpful discussions. We appreciate the engagement and the technical assistance of U. Frieß (FHI), C. Westphal, G. Hilgers, and V. Schimmang.

Support of the BMFT (Förderkennzeichen 05331 AXI/0)is gratefully acknowledged.

REFERENCES

1. A. Kastler; J. Phys. Radium 11, 255 (1950)
2. G. Lampel; Phys. Rev. Lett. 20, 491 (1968)
3. U. Fano; Phys. Rev. 178, 131 (1969), 184, 250 (1969)
4. Ch. Heckenkamp, F. Schäfers, G. Schönhense & U. Heinzmann; Phys. Rev. Lett. 52, 421 (1984)
5. A. Eyers, F. Schäfers, G. Schönhense, U. Heinzmann, H.P. Oepen, K. Hünlich, J. Kirschner & G. Borstel; Phys. Rev. Lett. 52, 1559 (1984)
6. F. Meier & D. Pescia in Optical Orientation, Modern Problems in Condensed Matter Sciences, Vol. 8, p. 295, F. Meier & B.P. Zakharchenya ed., Elsevier Science Publ., Amsterdam 1984
7. U. Heinzmann & G. Schönhense in Polarized Electrons in Surface Physics, p. 467 ff, R. Feder ed., World Scientific, Singapore 1985
8. For atoms: the intercombination lines (e.g. Hg: $6^3P \rightarrow 6^1S$) are allowed only by spin-orbit coupling,
   For solids: G. Borstel, M. Neumann & M. Wöhlecke; Phys. Rev. B 23, 3121 (1981)
9. M. Wöhlecke & G. Borstel in Optical Orientation, Modern Problems in Condensed Matter Sciences, Vol. 8, p. 423, F. Meier & B.P. Zakharchenya ed., Elsevier Science Publ., Amsterdam 1984
10. G. Borstel; Solid State Commun. 53, 87 (1985)
11. H.P. Oepen, K. Hünlich, J. Kirschner, A. Eyers, F. Schäfers, G. Schönhense & U. Heinzmann; Phys. Rev. B 31, 6846 (1985)
12. H.P. Oepen, K. Hünlich, J. Kirschner, A. Eyers & F. Schäfers; Solid State Commun. 59, 521 (1986)
13. We follow the sign convention used in Ref. 5,6; $P>0 \leftrightarrow \vec{P}/|P| = \vec{k}/|\vec{k}|$, $\vec{k}$ the wavevector of the outgoing electrons. The sign given in the data correspond to the selection rules for σ^+ circ. pol. light (dipole operator $\propto(x-iy)$, light propagation along -z, see Ref. 9).
14. J. Hermanson; Solid State Commun. 22, 9 (1977)
15. R. Raue, H. Hopster & R. Clauberg; Phys. Rev. Lett. 50, 1623 (1983)
16. R. Feder, W. Gudat, E. Kisker, A. Rodriguez & K. Schröder; Solid State Commun. 46, 619 (1983)
17. P. Bauer, W. Eckstein & N. Müller; Z. Phys. B 52, 185 (1983)
18. J. Noffke & L. Fritsche; J. Phys. F: Met. Phys. 12, 921 (1982)
19. J.F. van der Veen, F.J. Himpsel & D.E. Eastman; Phys. Rev. B 22, 4226 (1980)
20. G.D. Mahan; Phys. Rev. B 2, 4334 (1970)

21. R. Hora & M. Scheffler; Phys. Rev. B 29, 692 (1984)
22. J.U. Mack, E. Bertel, F.P. Netzer & D.R. Lloyd; Z. Phys. B 63, 97 (1986)
23. F. Schäfers, W. Peatman, A. Eyers, Ch. Heckenkamp, G. Schönhense & U. Heinzmann; Rev. Sci. Instruments 57, 1032 (1986)
24. See Ref. 23; we have used radiation with a vertical angle $|\psi|$ >0.75 mrad above/ below the orbit plane of the storage ring to get σ^+/σ^- polarized light.
25. K. Jost, J. Phys. E 12, 1006 (1979)
26. G. Haase & G. Schneider; Z. Phys. 144, 256 (1956)
27. A. Eyers, G. Schönhense, U. Frieß, F. Schäfers & U. Heinzmann; Surface Sci. 162, 96 (1985)
28. C. Kittel; Introduction to Solid State Physics, 5th Edition, p. 126, John Wiley & Sons, New York 1976
29. J.A. Knapp, F.J. Himpsel & D.E. Eastman; Phys. Rev. B 19, 4952 (1979)
30. G. Borstel; App. Phys. A 38, 193 (1985)
31. C.O. Almbladh & U. von Barth in Density Functional Methods in Physics, p. 209, R.M. Dreizler & J. da Providencia ed., Plenum Press, New York 1984
32. W. Speier, R. Zeller & J.C. Fuggle; Phys. Rev. B 32, 3597 (1985)
33. H. Wern, R. Courths, G. Leschik & S. Hüfner; Z. Phys. B 60, 293 (1985)
34. R. Courths, H.G. Zimmer, A. Goldmann & H. Saalfeld; Phys. Rev. B 34, 3577 (1986)
35. J. Noffke; private communication
36. H. Przybylski, A. Baalmann, G. Borstel & M. Neumann; Phys. Rev. B 27, 6669 (1983)
37. N.V. Smith; Phys. Rev. B 9, 1365 (1974)